Received: 18 September 2019 | Revised: 7 January 2020 | Accepted: 22 January 2020

DOI: 10.1111/jpi.12632

Check for updates

ORIGINAL ARTICLE

Journal of Pineal Research
Molecular, Biological, Physiological and Clinical Aspects of Melatonin

WILEY

Melatonin-stimulated exosomes enhance the regenerative potential of chronic kidney disease-derived mesenchymal stem/stromal cells via cellular prion proteins

Yeo Min Yoon[1] | **Jun Hee Lee**[1,2] | **Keon-Hyoung Song**[3] | **Hyunjin Noh**[4,5] | **Sang Hun Lee**[1,2]

[1]Medical Science Research Institute, Soonchunhyang University Seoul Hospital, Seoul, Korea

[2]Departments of Biochemistry, Soonchunhyang University College of Medicine, Cheonan, Korea

[3]Department of Pharmaceutical Engineering, College of Medical Science, Soonchunhyang University, Asan, Korea

[4]Department of Internal Medicine, Soonchunhyang University, Seoul, Korea

[5]Hyonam Kidney Laboratory, Soonchunhyang University, Seoul, Korea

Correspondence
Sang Hun Lee, Soonchunhyang Medical Science Research Institute, Soonchunhyang University Seoul Hospital, 59, Daesagwan-ro (657 Hannam-dong), Yongsan-gu, Seoul 140-887, Korea.
Email: ykckss1114@nate.com

Funding information
National Research Foundation of Korea, Grant/Award Number: NRF-2017M3A9B4032528 and NRF-2019M3A9H1103495

Abstract

Chronic kidney disease (CKD) is caused by dysfunctional kidneys, which result in complications like cardiovascular diseases. Chronic kidney disease-induced pathophysiological conditions decrease efficacy of autologous mesenchymal stem/stromal cell (MSC)-based therapy by reducing MSC functionality. To enhance therapeutic potential in patients with CKD, we isolated exosomes derived from melatonin-treated healthy MSCs (MT exosomes) and assessed the biological functions of MT exosome–treated MSCs isolated from patients with CKD (CKD-MSCs). Treatment with melatonin increased the expression of cellular prion protein (PrP^C) in exosomes isolated from MSCs through the upregulation of miR-4516. Treatment with MT exosomes protected mitochondrial function, cellular senescence, and proliferative potential of CKD-MSCs. MT exosomes significantly increased the level of angiogenesis-associated proteins in CKD-MSCs. In a murine hindlimb ischemia model with CKD, MT exosome–treated CKD-MSCs improved functional recovery and vessel repair. These findings elucidate the regenerative potential of MT exosome–treated CKD-MSCs via the miR-4516-PrP^C signaling axis. This study suggests that the treatment of CKD-MSCs with MT exosomes might be a powerful strategy for developing autologous MSC-based therapeutics for patients with CKD. Furthermore, miR-4516 and PrP^C could be key molecules for enhancing the regenerative potential of MSCs in ischemic diseases.

KEYWORDS

cellular prion protein, chronic kidney diseases, exosome, ischemic disease, melatonin, mesenchymal stem/stromal cells

1 | INTRODUCTION

Chronic kidney disease (CKD) is a major public health concern owing to its increasing prevalence (8%-16%) and associated complications including hypertension, atherosclerosis, aging, and diabetes.[1,2] Although kidney transplantation is the best strategy for improving kidney function, finding a matching donor is a limiting factor. Additionally, the long-lasting intense immunosuppression in kidney-transplanted patients with CKD leads to a high susceptibility to infection, malignancies, and cardiovascular diseases.[3]

© 2020 John Wiley & Sons A/S. Published by John Wiley & Sons Ltd

Furthermore, CKD-induced uremic toxins circulate in the serum of patients with CKD resulting in apoptosis of several vascular cells and the induction of vascular damage.[4] Since pharmacotherapy and kidney transplantation is incapable of improving the recovery and regeneration of the surrounding tissues affected by CKD, development of an effective therapeutic is imperative.

Mesenchymal stem/stromal cell (MSC)-based therapy finds utility in regenerative medicine due to its unique therapeutic potential, ease of isolation and expansion of MSCs from various tissues, ability to home to injured tissues, multipotency, and immune-modulatory effects.[5] There are over 600 clinical trials that have assessed the therapeutic efficacy of MSCs against several diseases (www.clinicaltrials.gov). Nevertheless, severe pathophysiological conditions like CKD and ischemia restrict the potency of autologous MSC-based therapy since patient condition decreases the quality and quantity of MSCs available for regeneration. Moreover, the mechanism by which MSCs affect several diseases remains unclear. Thus, it is important to develop a novel strategy for enhancing the function of patient-derived MSCs.

Various cells secrete membrane-bound vesicles, such as ectosomes, microvesicles, and exosomes, that are released into the extracellular space.[6] An increasing number of studies have shown that MSCs produce exosomes (50-200 nm diameter) that horizontally transfer messenger RNAs, microRNAs, and proteins to regulate a variety of functions in target cells in response to physiological and/or pathophysiological stimuli.[7,8] Mesenchymal stem/stromal cell-derived exosomes communicate with neighbor cells, maintain homeostasis within tissues, and regulate processes including cellular structure, inflammation, and metabolism.[7] Mesenchymal stem/stromal cell-derived exosomes have shown regenerative effects in several diseases such as cardiac fibrosis, myocardial infarction, neurodegeneration, stroke, skin wounds, limb ischemia, and various cancers.[8] Despite the accumulating evidence for MSC-derived exosomes in therapy, key questions pertaining to their mechanism of action remain unanswered. To treat human CKD with vascular complications, we isolated healthy human MSC-derived exosomes treated with melatonin (MT exosomes), that is an endogenous secretory hormone having therapeutic potential,[9] and investigated the activity of MSC-derived exosomes on patients with CKD-derived MSCs (CKD-MSCs). In this study, we detected the cellular prion protein (PrP^C) and hsa-miR-4516 in healthy human MSC-derived exosomes and determined their effect on mitochondria, CKD-derived senescence, proliferation, and secretion of angiogenic cytokines in CKD-MSCs. Furthermore, we assessed the effect of exosome-treated CKD-MSCs on neovascularization in a murine hindlimb ischemia model with CKD.

2 | MATERIALS AND METHODS

All experimental protocols have been described in detail in Appendix S1.

2.1 | Serum samples

The local ethics committee approved this study, and informed consent was obtained from all the individuals. Explanted sera (n = 37) were obtained from patients with CKD at the Seoul National University Hospital in Seoul, Korea (IRB: SCHUH 2018-04-035-002). Upon fulfilling transplantation criteria, the control samples were obtained from healthy patients (n = 40) at the National Cancer Center in Seoul, Korea (IRB: SCHUH 2018-04-035-002). Chronic kidney disease diagnoses were made based on abnormal kidney function with an estimated glomerular filtration rate (eGFR) <25 mL/min/1.73 m^2 over 3 months (stages 3b-5).

2.2 | Culturing healthy and CKD-MSCs

Human adipose tissue-derived MSCs were isolated from one healthy individual (healthy MSCs) and one patient with CKD (CKD-MSCs) from the Soonchunhyang University Seoul Hospital (IRB: SCHUH 2015-11-017 and SCHUH 2017-10-016). Chronic kidney disease was diagnosed in a patient with impaired kidney function and an estimated eGFR <35 mL/(min·1.73 m^2) for more than 3 months (stage 3b). Both types of isolates were positive for the MSC surface markers CD44 and Sca-1 and negative for CD45 and CD11b.[10] They also differentiated into chondrogenic, adipogenic, and osteogenic cells under specific media conditions.[10] Healthy and CKD-MSCs were transferred to α-Minimum Essential Medium (α-MEM; Gibco BRL) containing 10% (v/v) fetal bovine serum (FBS; Gibco BRL) and 100 U/mL penicillin/streptomycin (Gibco BRL) within 3 days and grown in a humidified 5% CO_2 incubator at 37°C.

2.3 | Isolation of MSC-derived exosomes

Exosomes from healthy and CKD-MSCs were extracted using an exosome isolation kit (Rosetta Exosome) and concentrated using centrifugal filters (Millipore).

2.4 | Treatment of CKD-MSCs with exosomes derived from healthy MSCs

CKD-MSCs were treated with 30 μg of exosomes derived from healthy MSCs for 24 hours. The concentration of exosomes was assessed using colorimetric BCA assay (Thermo Fisher Scientific).

2.5 | Quantification of microRNA (miRNA)

Healthy MSCs and their respective exosome preparations were used to extract total RNA (DNase digested) with the

miRNeasy Mini Kit (Qiagen). Quantitative real-time polymerase chain reaction (qRT-PCR) was performed using the TaqMan Small RNA Assay (Thermo Fisher Scientific) to determine the expression of miRNAs normalized to U6 rRNA or β-actin.

2.6 | SOD2 activity

Total protein was extracted from CKD-MSCs using a RIPA extraction buffer (Thermo Fisher Scientific). SOD2 activity was measured using a SOD activity kit (Enzo) as per the kit instructions. To inhibit SOD1 activity, 40 μg protein containing 2 mmol/L cyanide ion was added to each well. The absorbance was measured at 450 nm every minute for 15 minutes using a microplate reader (BMG Labtech), and activity was calculated according to the kit manual.

2.7 | Western blot analysis

Whole cell, cytosol, and mitochondrial fraction lysates were prepared from healthy and CKD-MSCs. These samples (30 μg protein each) were analyzed by sodium dodecyl sulfate-polyacrylamide gel electrophoresis using gels with porosity between 8% and 12% followed by transfer to a nitrocellulose membrane. After the blots were washed with TBST (10 mmol/L Tris-HCl [pH 7.6], 150 mmol/L NaCl, 0.05% Tween 20), they were blocked with 5% skim milk for 1 hour at room temperature followed by incubation with the following primary antibodies: p16 (clone no. D7C1M; cat. no. #80772; Cell Signaling Technology), p21 (clone no. WA-1; cat. no. sc-51689; Santa Cruz Biotechnology), SMP30 (clone no. 17; cat. no. sc-130344; Santa Cruz Biotechnology), p-Akt (Ser 473; cat. no. sc-101629; Santa Cruz Biotechnology), Akt (clone no. 281046; cat. no. MAB2055; R&D systems), p-ERK (clone no. E-4; cat. no. sc-7383; Santa Cruz Biotechnology), ERK (clone no. 216703; cat. no. MAB1576; R&D systems), p-FAK (Tyr 576-R; cat. no. sc-16563-R; Santa Cruz Biotechnology), FAK (clone no. OTI4D11; cat. no. NBP2-45923), p-Src (clone no. E-4; cat. no. sc-7383; Santa Cruz Biotechnology), Src (clone no. 327 537; cat. no. MAB3389; R&D systems), CD81 (clone no. B-11; cat. no. sc-166029; Santa Cruz Biotechnology), CD63 (clone no. MX-49.129.5; cat. no. sc-5275; Santa Cruz Biotechnology), GP78 (clone no. F-3; cat. no. sc-166358; Santa Cruz Biotechnology), PrP^C (clone no. H8; cat. no. sc-393165; Santa Cruz Biotechnology), ubiquitin (clone no. Ubi-1; cat. no. NB300-130; NOVUS, Littleton), and β-actin (Santa Cruz Biotechnology). The membranes were then washed and incubated with the respective goat anti-rabbit IgG or goat anti-mouse IgG secondary antibodies (Santa Cruz Biotechnology). The blots were developed using enhanced chemiluminescence (Amersham Pharmacia Biotech).

2.8 | Senescence β-galactosidase (SA-β-gal) cell staining

Healthy and CKD-MSCs (with or without melatonin treatment) were cultured in 24-well plates (5000 cells/well) and assayed using the Senescence β-Galactosidase Staining kit (Cell Signaling Technology) following the kit protocol. Development of blue color was observed by light microscopy (Olympus).

2.9 | Single-cell expansion assay

Healthy and CKD-MSC suspensions containing 10^3 cells in 10 mL complete medium were diluted 1:10 (cells:complete medium), and 100 μL of the dilutions (~1 cell/100 μL) was-seeded into a 96-well plate. The cells were cultured upon treatment with PBS, Con exosomes, MT exosomes, MT exosomes+si*PRNP*, and MT exosomes+si*Scr* in a humidified incubator. Each well was examined for growth on day 10.

2.10 | Kinase assays for complex I and IV activity

Protein lysates (30-50 μg) were assayed for the activity of complex I and IV (Abcam). Activation of complex I and IV was quantified by measuring absorbance at 450 nm on a microplate reader (BMG Labtech).

2.11 | Human angiogenesis protein array

Levels of angiogenesis-associated proteins in CKD-MSCs treated with PBS, Con exosomes, and MT exosomes were determined using the Human Angiogenesis Antibody Array (Abcam). Total protein lysates (200 μg) were suspended in bovine serum albumin (blocking buffer provided) and assayed as per the kit protocol.

2.12 | Ethics statement

All animal care procedures and experiments were approved by the Institutional Animal Care and Use Committee of Soonchunhyang University Seoul Hospital (IACUC2013-5) and were performed in accordance with the National Research Council (NRC) Guidelines for the Care and Use of Laboratory Animals. The 8-week-old male BALB/c nude mice (Biogenomics) were maintained on a 12-hour light/dark cycle at 25°C in accordance with the Soonchunhyang University Seoul Hospital regulations.

2.13 | Murine hindlimb ischemia model with CKD

Eight-week-old male BALB/c nude mice were fed an adenine-containing diet (0.75% adenine) for 1-2 weeks, and body weights were measured weekly. The mice were randomly distributed to four groups consisting of 10 mice each. Blood was stored at −80°C for measuring blood urea nitrogen and creatinine posteuthanasia. To understand vascular disease and assess neovascularization in CKD, a murine hind limb ischemia model with CKD was established after adenine-loaded feeding for 1 week. Ischemia was induced by ligation and excision of the proximal femoral artery and boundary vessels of the CKD mice. Within 6 hours of the surgical procedure, cells were injected into ischemic sites (10^6 cells/100 μL of PBS/mouse; single injection; 5 mice/treatment group) of the CKD mice. Blood perfusion was calculated by the ratio of blood flow in the ischemic (left) limb to that in the nonischemic (right) limb on postoperative days 0, 7, 14, 21, and 28 using laser Doppler perfusion imaging (LDPI; Moor Instruments).

2.14 | Immunohistochemical staining

Ischemic thigh tissues were removed on postoperative days 3 and 28, fixed with 4% paraformaldehyde (Sigma), and each tissue sample was embedded in paraffin. For measuring

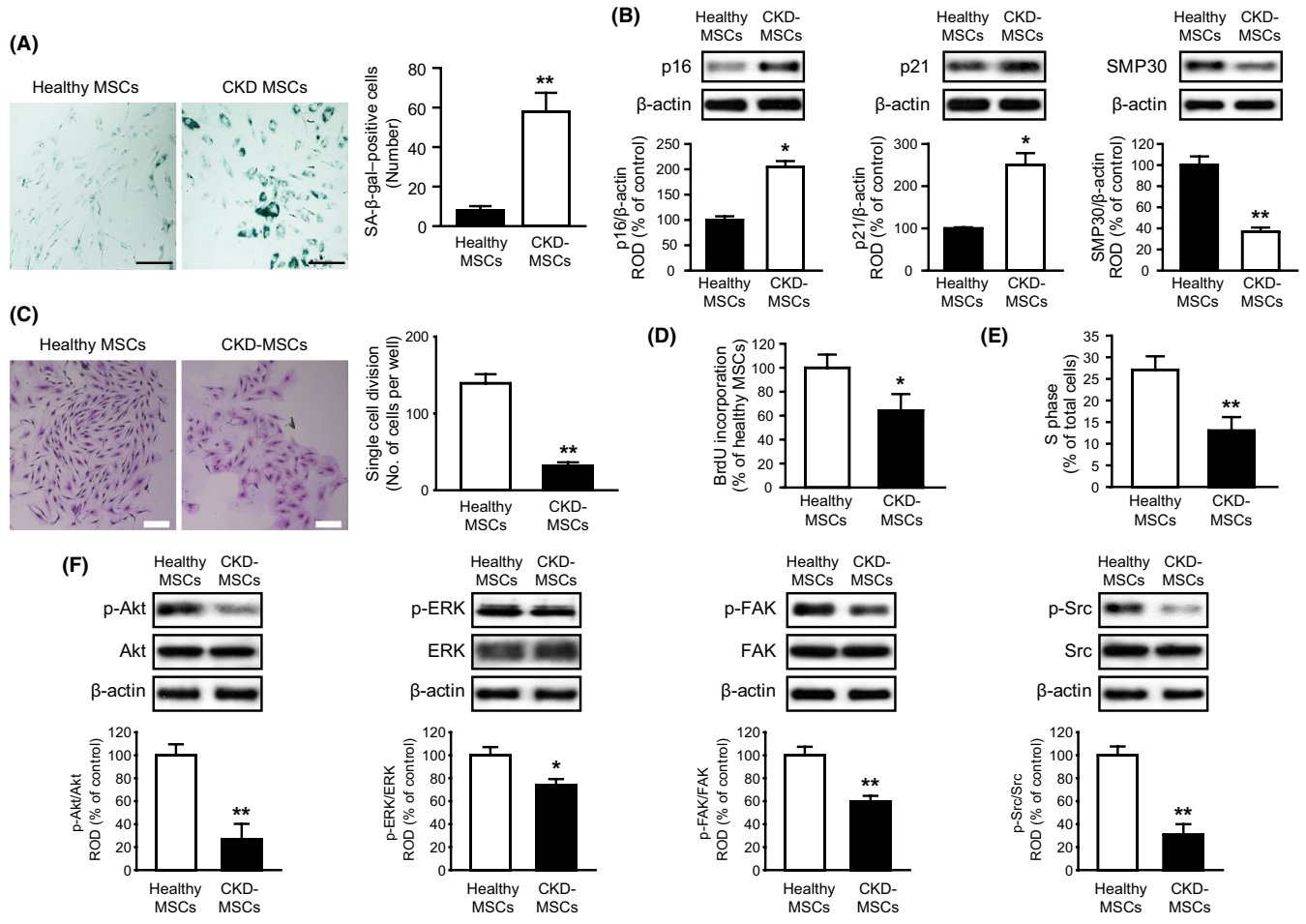

FIGURE 1 Effect of chronic kidney disease (CKD) on the biological functions in MSCs. A, Senescence-associated β-galactosidase (SA-β-gal) staining in MSCs derived from healthy individuals (healthy MSCs) and patients with CKD (CKD-MSCs) (n = 5). Scale bar = 100 μm. Cellular senescence was determined by the number of SA-β-gal–positive cells. The values represent mean ± standard error of the mean (SEM), $^{**}P < .01$. B, The expression of p16, p21, and SMP30 in healthy MSCs and CKD-MSCs (n = 3). The protein levels were quantified by densitometry and normalized to β-actin levels. The values represent mean ± SEM, $^{*}P < .05$, $^{**}P < .01$. C, Single-cell expansion assay in healthy and CKD-MSCs (n = 5). Scale bar = 100 μm. Proliferative potential was determined by the number of cells that migrated toward the periphery of the culture dish. The values represent mean ± SEM, $^{**}P < .01$. D, BrdU incorporation in healthy and CKD-MSCs (n = 5). The values represent the means ± SEM. $^{*}P < .05$. E, S-phase flow cytometry (n = 5) analysis for healthy and CKD-MSCs. The values represent mean ± SEM, $^{**}P < .01$. F, Levels of p-Akt, p-ERK, p-FAK, and p-Src in healthy and CKD-MSCs (n = 3). The proteins were quantified by densitometry normalized to total Akt, ERK, FAK, and Src levels, respectively. The values represent mean ± SEM, $^{*}P < .05$, $^{**}P < .01$

apoptosis and proliferation, the tissues were stained for TUNEL (Trevigen) and PCNA (Santa Cruz Biotechnology), respectively. Immunofluorescence staining was performed with primary antibodies against CD11b (Abcam), CD31 (Santa Cruz Biotechnology), and α-SMA (alpha-smooth muscle actin; Santa Cruz Biotechnology) followed by secondary antibodies conjugated with Alexa Fluor 488 or 594 (Thermo Fisher Scientific). Nuclei were stained with 4′,6-diamidino-2-phenylindole (Sigma), and the samples were examined by confocal microscopy (Olympus).

2.15 | Statistical analysis

Two-tailed Student's *t* test and one- or two-way analysis of variance were used to calculate significance between groups, and the results were expressed as standard error of mean (SEM). Comparisons between three or more groups were made using Dunnett's or Tukey's post hoc test. Data were considered significantly different at $P < .05$.

3 | RESULTS

3.1 | CKD decreased the bioactivity of MSCs

We isolated MSCs from healthy individuals (healthy MSCs) and patients with CKD (CKD-MSCs) to determine the effect of CKD on MSC functionality. SA-β-gal staining showed that cellular senescence was significantly increased in CKD-MSCs compared with that in healthy MSCs (Figure 1A). In CKD-MSCs, pro-senescent proteins p16 and p21 were significantly increased and the anti-senescent marker SMP30 was significantly decreased (Figure 1B). Single-cell expansion assays showed that CKD decreased MSC proliferation (Figure 1C). BrdU incorporation assay and S-phase flow cytometry analysis also revealed that the proliferation of MSCs was inhibited by CKD (Figure 1D,E). To explore CKD-mediated alteration of cellular signaling, activation of the following signaling pathways was assessed: Akt for survival; ERK for proliferation; FAK for migration; and Src for angiogenesis. These proteins were significantly phosphorylated in CKD-MSCs compared with those in healthy MSCs (Figure 1F). These results indicate that CKD deteriorates MSC function.

3.2 | Melatonin increased the level of PrP^C in MSC-derived exosomes

Compared with healthy individuals, patients with CKD had significantly lower serum concentration of PrP^C (Figure S1, Figure 2A). To investigate the effect of melatonin on PrP^C levels in healthy MSCs and CKD-MSCs, both cells were treated with melatonin and the levels of PrP^C were assayed in cell lysates and exosomes. Melatonin significantly increased the expression of PrP^C in both lysates and exosomes of healthy MSCs and CKD-MSCs (Figure 2B). Moreover, the expression of PrP^C in CKD-MSCs significantly increased upon treatment with MT exosomes (Figure S2, Figure 2C). These results indicate that MT exosomes enhanced the expression of PrP^C in CKD-MSCs. To understand how PrP^C expression is regulated by MT exosomes, we performed an miRNA microarray assay in Con exosomes and MT exosomes (Figure 2D). The heat map showed that miR-4516, miR-6794-5p, and miR-6806-3p were significantly increased in MT exosomes (Figure S3A, Figure 2E). Based on the heat map result, some miRNAs, such as miR-4516, Let-7b-5p, miR-548ac, miR-6794-5p, miR-6806-3p, and miR-6868-3p, were involved in gene regulation for vascular formation and cell proliferation. Although Let-7b-5p and miR-6794-5p showed a similar expression profile to miR-4516 in healthy and CKD-MSCs treated with melatonin, the increase in Let-7b-5p and miR-6794-5p were significantly lower than the increase in miR-4516 (Figure S3B). Furthermore, other miRNAs, including miR-548ac, miR-6806-3p, and miR-6868-3p, did not show the significant difference of gene expression in healthy and CKD-MSCs treated with melatonin (Figure S3B). We wanted to delineate the role(s) of miR-4516 on the expression of PrP^C. Melatonin drastically increased the expression of miR-4516 in healthy MSCs (Figure 2F). Additionally, PrP^C levels were significantly increased in MT exosomes, whereas inhibition of miR-4516 suppressed the expression of PrP^C in MT exosomes (Figure 2G). Furthermore, treatment with MT exosomes significantly augmented the level of PrP^C in CKD-MSCs while inhibition of miR-4516 blocked MT exosome–mediated expression of PrP^C (Figure 2H). In addition, overexpression of miR-4516 significantly increased the level of PrP^C in healthy MSCs, CKD-MSCs, and exosomes derived from healthy MSCs, whereas inhibition of miR-4516 significantly reduced the expression of PrP^C in healthy MSCs, CKD-MSCs, and exosomes derived from healthy MSCs (Figure S4). To further investigate how miR-4516 regulates the expression of PrP^C, the level of GP78 was assessed via expression of miR-4516. Our previous study has shown that the level of PrP^C is regulated by GP78 which is an membrane-anchored E3 ligase.[11] Inhibition of miR-4516 significantly increased the expression of GP78, resulting in augmentation of ubiquitination of PrP^C (Figure S5A-D). However, this effect was blocked by over expression of miR-4516 (Figure S5A-D). Moreover, the level of GP78 was significantly decreased in treatment of CKD-MSCs with MT exosomes, whereas the level of GP78 was not decreased by MT exosomes treated

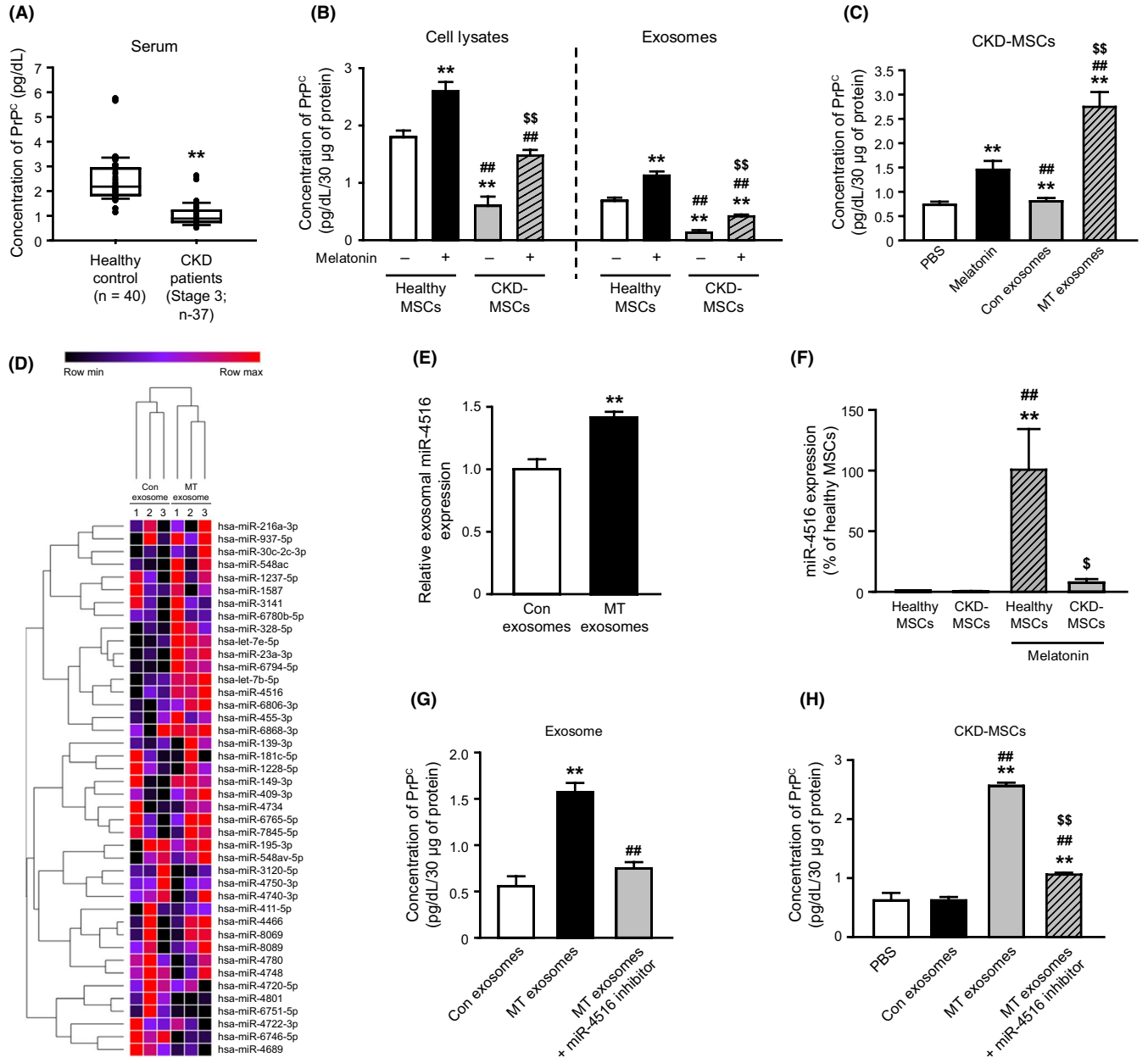

FIGURE 2 Melatonin increases the level of cellular prion protein (PrP^C) in MSC-derived exosomes via upregulation of miR-4516. A, Concentration of PrP^C in serum of healthy individuals (n = 40) and patients with CKD (stage 3; n = 37) as measured by ELISA. The values represent mean ± SEM, $^{**}P < .01$. B, The level of PrP^C in cell lysates and exosomes from healthy and CKD-MSCs (n = 3) as measured by ELISA. The values represent mean ± SEM, $^{**}P < .01$ compared with healthy MSCs; $^{\#\#}P < .01$ compared with healthy MSCs treated with melatonin; $^{\$\$}P < .01$ compared with untreated CKD-MSCs. C, Levels of PrP^C in CKD-MSCs after treatment with melatonin, exosomes derived from healthy MSCs (Con exosomes), and exosomes derived from melatonin-treated healthy MSCs (MT exosomes) (n = 3) as measured by ELISA. The values represent mean ± SEM, $^{**}P < .01$ compared with PBS; $^{\#\#}P < .01$ compared with melatonin-treated; $^{\$\$}P < .01$ compared with Con exosomes. D, Hierarchical clustering showing differential miRNA expression in Con exosomes and MT exosomes. E, The expression of miR-4516 in Con exosomes and MT exosomes (n = 3) as measured by real-time PCR. The values represent mean ± SEM, $^{**}P < .01$. F, miR-4516 levels in healthy MSCs and CKD-MSCs after treatment with melatonin (n = 3) as measured by real-time PCR. The values represent mean ± SEM, $^{**}P < .01$ compared with untreated healthy MSCs; $^{\#\#}P < .01$ vs untreated CKD-MSCs; $^{\$\$}P < .01$ compared with melatonin-treated healthy MSCs. G, Levels of PrP^C in MT exosomes with/without miR-4516 inhibitor (n = 5) as measured by ELISA. The values represent mean ± SEM, $^{**}P < .01$ compared with Con exosomes; $^{\#\#}P < .01$ compared with MT exosomes. H, PrP^C expression in CKD-MSCs after treatment with Con exosomes and MT exosomes (n = 5) as measured by ELISA. The values represent mean ± SEM, $^{**}P < .01$ compared with PBS; $^{\#\#}P < .01$ compared with Con exosomes; $^{\$\$}P < .01$ compared with MT exosomes

with miR-4516 inhibitor (Figure S5E,F). These findings indicate that the levels of PrP^C in both exosomes and exosome-treated CKD-MSCs are regulated by melatonin-induced miR-4516 expression.

3.3 | MT exosomes rescued CKD-induced mitochondrial dysfunction

To determine the effect of MT exosomes on mitochondrial dysfunction in CKD-MSCs, mitochondrial morphology was analyzed in MT exosome–treated CKD-MSCs (Figure 3A). The number of abnormal mitochondria significantly decreased upon treatment MT exosomes (Figure 3B). Compared with the PBS- or Con exosome–treated samples, mitochondrial complex I and IV and SOD2 activities were significantly enhanced in CKD-MSCs upon treatment with MT exosomes (Figure 3C-E). Moreover, production of ROS in mitochondria was significantly suppressed in MT exosome–treated CKD-MSCs (Figure 3F). Knockdown of *PRNP* inhibited these phenotypes exhibited by MT exosomes in CKD-MSCs (Figure 3C-F). These results indicate that MT exosomes protect mitochondrial dysfunction in CKD-MSCs via the upregulation of PrP^C.

3.4 | MT exosomes protected cellular senescence in CKD-MSCs

To examine whether MT exosomes rescue CKD-mediated cellular senescence in MSCs, we performed SA-β-gal staining using MT exosome–treated CKD-MSCs (Figure 4A). We observed a decreased number of SA-β-gal–positive CKD-MSCs upon treatment with MT exosomes (Figure 4B). The levels of pro-senescent proteins p16 and p21 decreased, and the anti-senescent marker SMP30 increased in MT exosome–treated CKD-MSCs (Figure 4C,D). The protective effect of MT exosomes on CKD-induced cellular senescence in MSCs was blocked by silencing *PRNP* (Figure 4A-D). These results indicate that treatment with MT exosomes rescues CKD-mediated cellular senescence of MSCs.

3.5 | MT exosomes increased proliferation and secretion of angiogenic cytokines in CKD-MSCs

Further, we investigated the effect of MT exosomes on CKD-MSC proliferation (Figure 5A) and observed that MT exosome–treated CKD-MSCs were more proliferative whereas

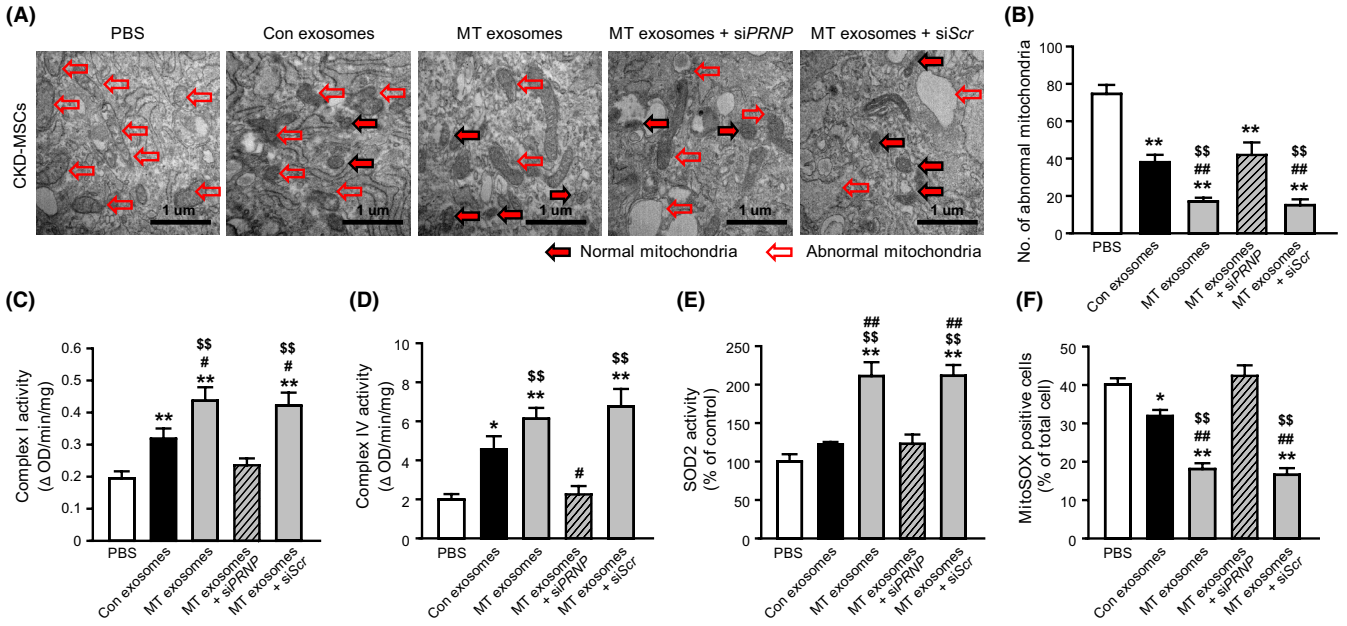

FIGURE 3 Effect of MT exosomes on mitochondrial function in CKD-MSCs via expression of PrP^C. A, Representative TEM images of mitochondria in CKD-MSCs after treatment with exosomes. Scale bar = 1 μm. B, Percentage of abnormal mitochondria obtained from a TEM image (n = 3). The values represent mean ± SEM, $^{**}P < .01$ compared with PBS; $^{\#\#}P < .01$ compared with Con exosomes; $^{\$\$}P < .01$ compared with MT exosomes treated with siRNA against *PRNP* (MT exosomes + si*PRNP*). C-E, Activities of mitochondrial complex I (C) and IV (D) and SOD2 (E) in exosome-treated CKD-MSCs (n = 3). The values represent mean ± SEM, $^{*}P < .05$, $^{**}P < .01$ compared with PBS; $^{\#}P < .05$, $^{\#\#}P < .01$ compared with Con exosomes; $^{\$\$}P < .01$ compared with MT exosomes + si*PRNP*. F, MitoSOX-positive cells quantified by flow cytometry in exosome-treated CKD-MSCs (n = 5). The values represent mean ± SEM, $^{*}P < .05$, $^{**}P < .01$ compared with PBS; $^{\#\#}P < .01$ compared with Con exosomes; $^{\$\$}P < .01$ compared with MT exosomes + si*PRNP*

knockdown of *PRNP* hampered this proliferative capacity (Figure 5B). To further explore the effect of MT exosomes on cell signaling in CKD-MSCs, activation of Akt, ERK, FAK, and Src was assayed by Western blot analysis (Figure 5C). Treatment of CKD-MSCs with MT exosomes showed an increase in the phosphorylated forms of Akt, ERK, FAK, and Src (Figure 5D). Consistent with our previous results, silencing PRNP in the MT exosomes significantly reduced the levels of these phosphorylated proteins (Figure 5D). To verify whether MT exosomes augment the expression of angiogenic cytokines in CKD-MSCs, a human angiogenesis protein array was performed using Con- and MT-exosome–treated CKD-MSCs (Figure S6 and Figure 6A). The levels of VEGFR2, VEGFR3, IL-1α, I-TAC, MCP-3, MCP-4, MMP-1, MMP-9, and uPAR were significantly increased in MT exosome–treated CKD-MSCs compared with those in Con exosome–treated CKD-MSCs (Figure 6A,B). These results demonstrate that MT exosomes enhance the proliferative and angiogenic potential of CKD-MSCs.

3.6 | MT exosome–treated CKD-MSCs improved the functional recovery in a murine hindlimb ischemia model with CKD

A murine hindlimb ischemia model with CKD was established to investigate whether MT exosome–treated CKD-MSCs enhance neovascularization (Figure S7). On postoperative day 3, survival and proliferation of transplanted MSCs were significantly increased in the animals injected with MT exosome–treated CKD-MSCs compared with that in other groups (Figure 7A,B). On postoperative day 28, the blood perfusion ratio and percentage of limb salvage were significantly higher in limbs transplanted with MT exosome–treated CKD-MSCs than with any other treatment (Figure 7C-F). Immunofluorescence staining for CD31 (capillary) and α-SMA (arterioles) showed that the densities of capillaries and arterioles were significantly increased in mice transplanted with MT exosome–treated CKD-MSCs (Figure 7G,H). However, silencing of *PRNP* significantly suppressed this MT exosome–mediated functional recovery and neovascularization. These results indicate that MT exosome–treated CKD-MSCs enhance functional recovery in a murine hindlimb ischemia model with CKD by upregulating PrP^C.

4 | DISCUSSION

CKD induces the progressive loss of function in kidneys resulting in ineffective homeostasis in the body. CKD-induced uremic toxins, such as indoxyl sulfate and p-cresol, hamper the biological activities of MSCs and lead to cardiovascular disease, weakened bones, malfunctioning central nervous

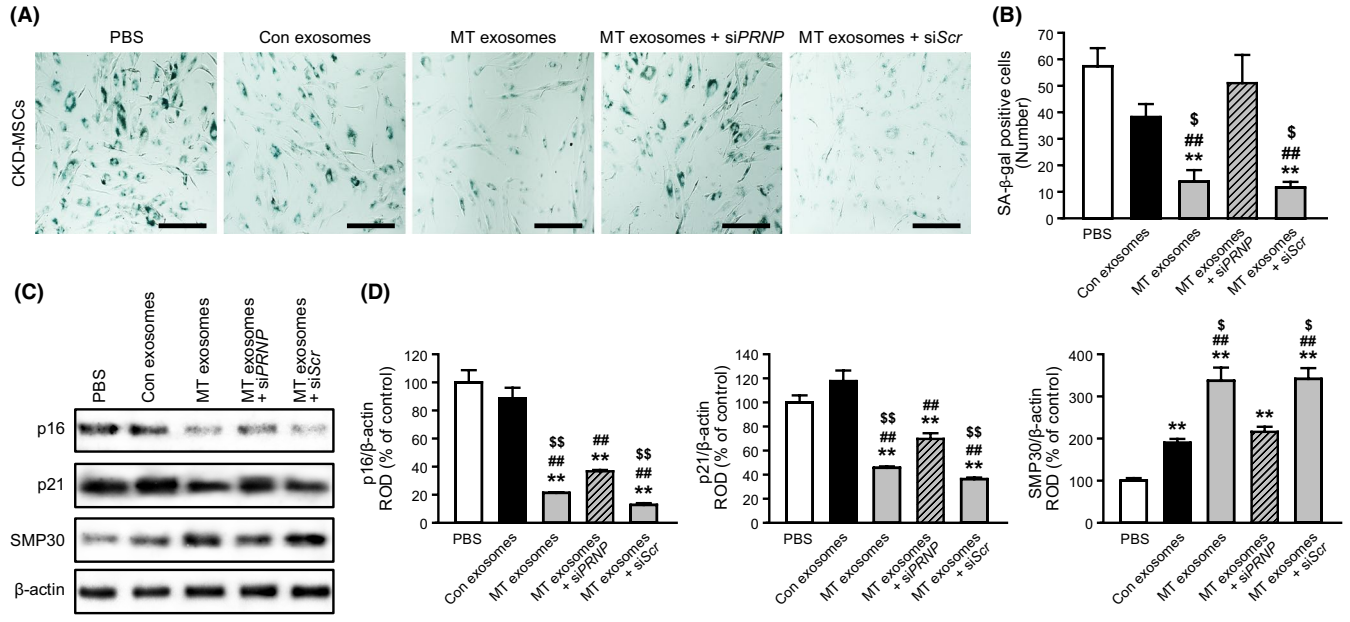

FIGURE 4 MT exosomes protect cellular senescence in CKD-MSCs by upregulating PrP^C. A, SA-β-gal staining in CKD-MSCs treated with exosomes. B, Cellular senescence was determined by the number of SA-β-gal–positive cells (n = 5). Scale bar = 100 μm. The values represent mean ± standard error of the mean (SEM), $^{**}P < .01$ compared with PBS; $^{\#\#}P < .01$ compared with Con exosomes; $^{\$}P < .05$ compared with MT exosomes + si*PRNP*. C, The expression of p16, p21, and SMP30 in CKD-MSCs treated with exosomes. D, Protein levels were quantified by densitometry normalized to β-actin levels (n = 3). The values represent mean ± SEM, $^{**}P < .01$ compared with PBS; $^{\#\#}P < .01$ compared with Con exosomes; $^{\$}P < .05$, $^{\$\$}P < .01$ compared with MT exosomes + si*PRNP*

system, and improper inflammation in patients.[12,13] The regenerative potential of CKD-MSCs is also suppressed in a murine ischemic injury.[10,14] Consistent with these findings, our results have shown that biological functions like senescence, proliferation, and mitochondrial activity were significantly decreased in CKD-MSCs and treatment with MT exosomes

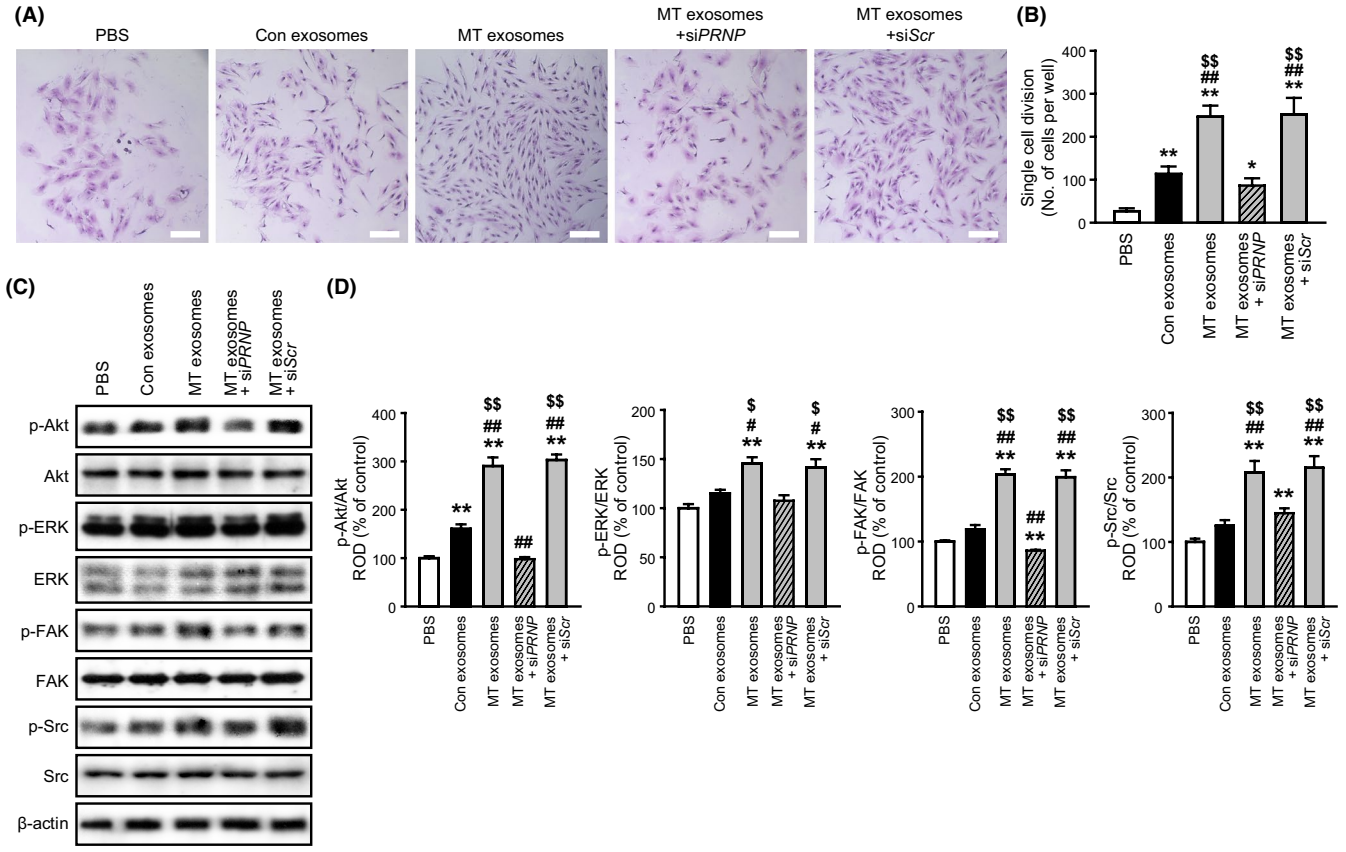

FIGURE 5 Effect of MT exosomes on proliferation and cellular signaling in CKD-MSCs. A, Single-cell expansion assay in CKD-MSCs treated with exosomes. Scale bar = 100 μm. B, The number of expanded cells in CKD-MSCs treated with exosomes (n = 5). The values represent mean ± SEM. $^{**}P < .01$ compared with PBS; $^{\#\#}P < .01$ compared with Con exosomes; $^{\$\$}P < .01$ compared with MT exosomes + si*PRNP*. C, Levels of p-Akt, p-ERK, p-FAK, and p-Src in CKD-MSCs treated with exosomes. D, The proteins were quantified by densitometry normalized to total Akt, ERK, FAK, and Src levels, respectively. The values represent mean ± SEM, $^{*}P < .05$, $^{**}P < .01$ compared with PBS; $^{\#}P < .05$, $^{\#\#}P < .01$ compared with Con exosomes; $^{\$}P < .05$, $^{\$\$}P < .01$ compared with MT exosomes + si*PRNP*

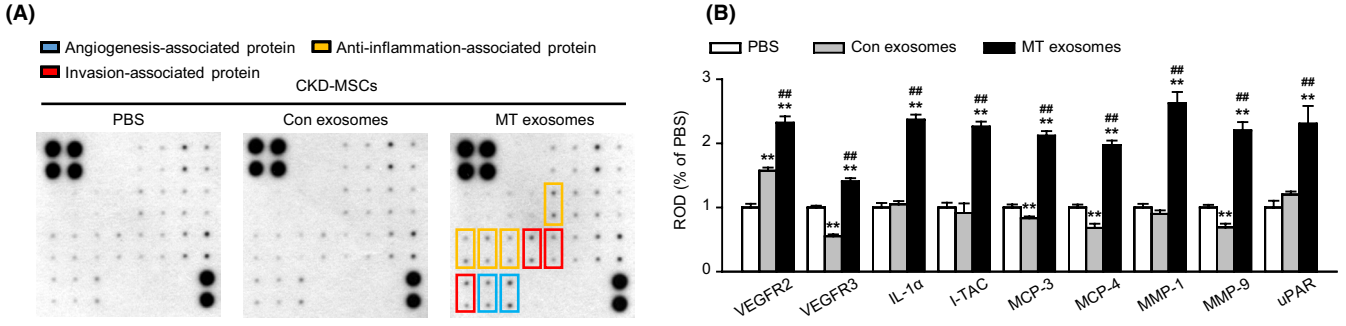

FIGURE 6 Expression of angiogenesis-mediated proteins in MT exosome–treated CKD-MSCs. A, Dot-blot analysis of angiogenesis-mediated proteins in CKD-MSCs treated with PBS, Con exosomes, and MT exosomes. A detailed map of the human angiogenesis protein array is in Figure S7. B, The levels of vascular endothelial growth factor receptor 2 (VEGFR2; 2nd row, 7-8 line; blue box), VEGFR3 (3rd row, 7-8 line; blue box), interleukin 1 alpha (IL-1α; 5th row, 3-4 line; yellow box), interferon-inducible T-cell alpha chemoattractant (I-TAC; 1st row, 5-6 line; yellow box), monocyte-chemotactic protein 3 (MCP-3; 2nd row, 5-6 line; yellow box), MCP-4 (3rd row, 5-6 line; yellow box), matrix metalloproteinase-1 (MMP-1; 4th row, 5-6 line; red box), MMP-9 (5th row, 5-6 line; red box), and urokinase receptor (uPAR; 1st row, 7-8 line; red box) in CKD-MSCs treated with PBS, Con exosomes, and MT exosomes (n = 6). The values represent mean ± SEM, $^{**}P < .01$ compared with PBS; $^{\#\#}P < .01$ compared with Con exosomes

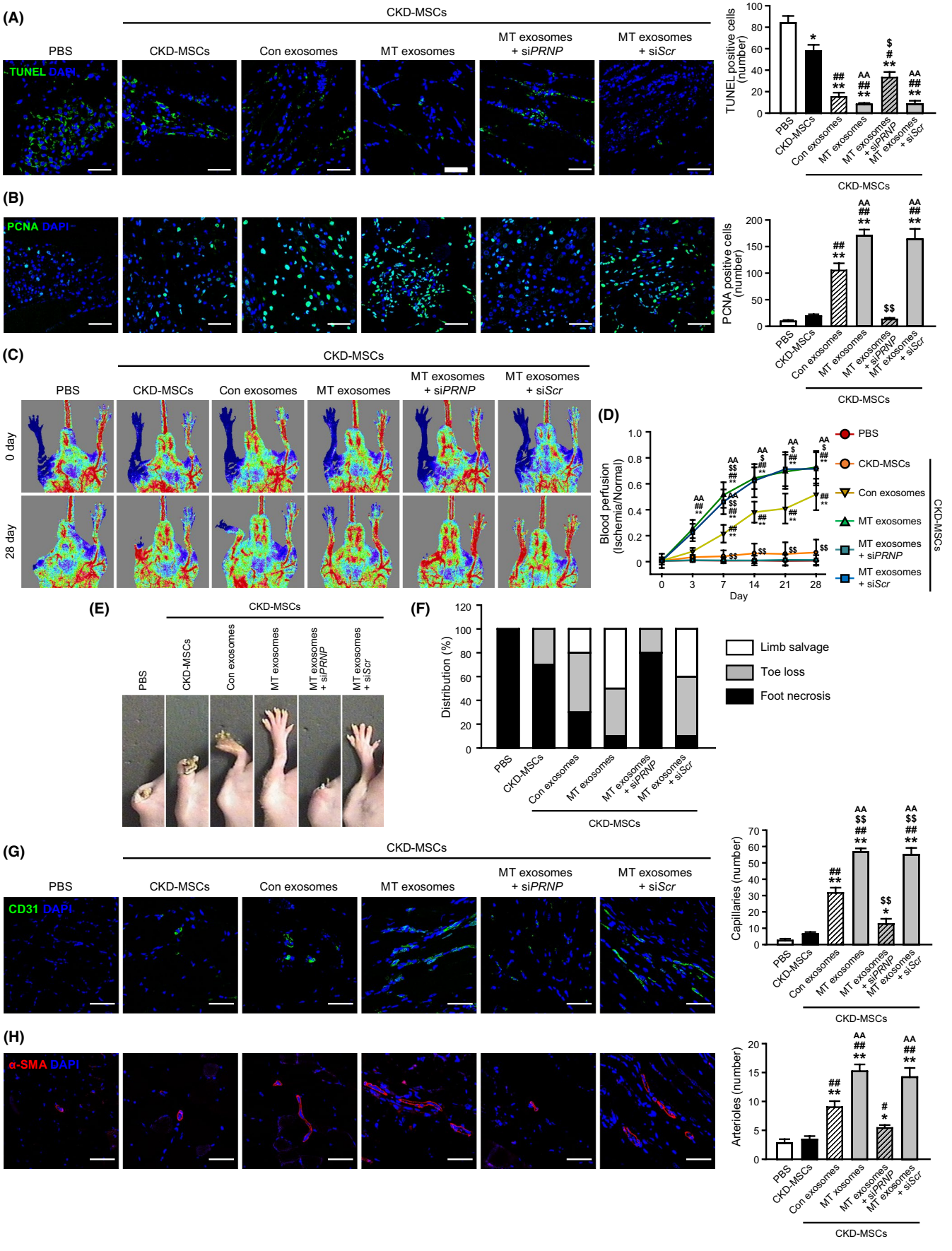
(A)
CKD-MSCs
PBS
CKD-MSCs
Con exosomes
MT exosomes
MT exosomes + siPRNP
MT exosomes + siScr
TUNEL DAPI
TUNEL positive cells (number)
(B)
PCNA DAPI
PCNA positive cells (number)
(C)
0 day
28 day
(D)
Blood perfusion (Ischemia/Normal)
Day
(E)
(F)
Distribution (%)
Limb salvage
Toe loss
Foot necrosis
(G)
CD31 DAPI
Capillaries (number)
(H)
α-SMA DAPI
Arterioles (number)

FIGURE 7 MT exosome–treated CKD-MSCs increase the functional recovery in a murine hindlimb ischemia model with CKD. A and B, TUNEL staining (A) and immunofluorescence staining for PCNA (B) using day 3 ischemic limb tissues (n = 5). Scale bar = 50 μm. The values represent mean ± SEM, $^{*}P < .05$, $^{**}P < .01$ compared with PBS; $^{\#}P < .05$, $^{\#\#}P < .01$ compared with CKD-MSCs; $^{\$}P < .05$, $^{\$\$}P < .01$ compared with CKD-MSCs + Con exosomes; $^{AA}p < 0.01$ compared with CKD-MSCs + MT exosomes. C, Laser Doppler perfusion imaging (LDPI) analysis of the ischemic limbs of CKD mice transplanted with CKD-MSCs treated with exosomes. D, Blood perfusion ratios as analyzed by LDPI (n = 10). The values represent mean ± SEM, $^{**}P < .01$ compared with PBS; $^{\#\#}P < .01$ compared with CKD-MSCs; $^{\$}P < .05$, $^{\$\$}P < .01$ compared with CKD-MSCs + Con exosomes; $^{AA}p < 0.01$ compared with CKD-MSCs + MT exosomes. E, Representative images illustrating various experimental outcomes (foot necrosis, toe loss, or limb salvage) in ischemic limbs on day 28 after surgery. F, Distribution of different outcomes on postoperative day 28 (n = 10). G and H, Immunofluorescence staining for CD31 (G; green) and α-SMA (H; red) on postoperative day 28 in ischemic limb tissues. Scale bar = 50 μm. Standard quantification of the capillary (G) and arteriole density (H) was calculated as the number of CD31- and α-SMA–positive cells (n = 5). The values represent mean ± SEM, $^{*}P < .05$, $^{**}P < .01$ compared with PBS; $^{\#}P < .05$, $^{\#\#}P < .01$ compared with CKD-MSCs; $^{\$\$}P < .01$ compared with CKD-MSCs + Con exosomes; $^{AA}p < 0.01$ compared with CKD-MSCs + MT exosomes

drastically improved these CKD-mediated pathophysiological conditions. Since exosomes are one-way conveyors of cellular components like nucleic acids, proteins, and lipids from the donor to the recipient cells to regulate recipient cellular process(es), it is crucial to understand the role(s) of the complex cargo in exosomes.[7] This study shows that melatonin increased the expression of PrP^C in MSC-derived exosomes, suggesting that exosomal PrP^C is an important component for enhancing the function of recipient CKD-MSCs.

Several studies have reported that PrP^C improves the regenerative potential of MSCs and is used as a cell-based therapeutic against various diseases.[10,14,15] PrP^C, a highly conserved and ubiquitous glycoprotein, regulates anti-oxidative and immunomodulatory effects, neovascularization, mitochondrial function, cellular senescence, apoptosis, and proliferation in MSCs against ischemia-induced oxidative stress.[10,14,15] Our results show that the expression of PrP^C was significantly increased MT exosomes and MT exosome–treated CKD-MSCs. Several studies have reported that microRNAs from MSC-derived exosomes, such as miR-22, miR-125a, miR-133b, and miR-146b, rescue myocardial infarction,[16] endothelial cell angiogenesis,[17] stroke,[18] and inhibit tumor growth.[19] Other studies have demonstrated that exosomes isolated from MSCs contain cystinosin,[20] neprilysin,[21] and CD73[22] and have shown efficacy against cystinosis, Alzheimer's diseases, and graft-versus-host disease, respectively. A few studies have revealed that the exosomes secreted by melatonin-treated adipocytes contain elevated levels of α-ketoglutarate resulting in the alleviation of metabolic inflammation.[23] To the best of our knowledge, this study is the first to reveal that exosomes isolated from melatonin-treated MSCs contained higher levels of PrP^C and MT exosomes enhanced the function of CKD-MSCs thereby improving neovascularization in a murine hindlimb ischemia model with CKD. These findings suggest that PrP^C could be a major target for developing MSC-derived exosome-mediated pharmacotherapeutics.

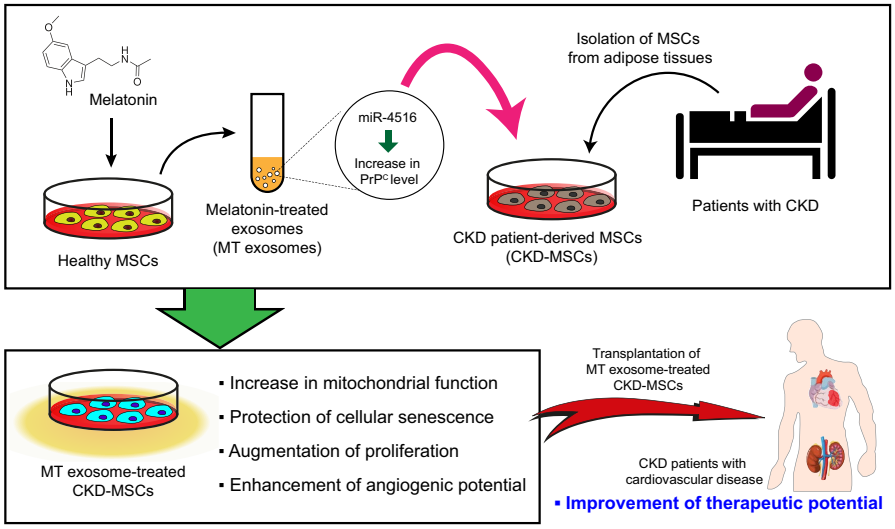

FIGURE 8 Schematic representation of the proposed mechanisms by which exosomes isolated from melatonin-treated healthy MSCs (MT exosomes) enhances the functionality of CKD-MSCs via the miR-4516-PrP^C signal axis. Melatonin increases the expression of PrP^C in exosomes derived from healthy MSCs via miR-4516. Treatment with MT exosomes increases mitochondrial function, cellular proliferation, and expression of angiogenesis-associated proteins in CKD-MSCs and decreases CKD-induced cellular senescence by upregulating PrP^C thereby improving functional recovery and neovascularization in ischemic diseases with CKD

Using miRNA profiling analysis, we have identified that melatonin increases the expression of hsa-miR-4516, a major player in the regulation of PrP^C expression, in MSC-derived exosomes. Some studies have shown that miR-4516 is involved in autophagy[24] and is a potential biomarker for dust-induced pulmonary fibrosis.[25] A recent study has revealed miR-4516 as a novel therapeutic target against glioblastoma.[26] Our results show that melatonin increased the levels of MSC-derived exosomal miR-4516 whose inhibition significantly decreased PrP^C levels in MT exosomes and MT exosome–treated CKD-MSCs. These findings indicate that miR-4516 increases PrP^C expression in MSCs and MT exosomes resulting in the rescue of CKD-MSCs cellular activities, such as mitochondrial function, CKD-mediated senescence, proliferation, and secretion of angiogenic cytokines, via the exosome/miR-4516/PrP^C axis. To our belief, this is the first report to indicate a novel function of melatonin-induced hsa-miR-4516 that regulates the expression of PrP^C in MSC-derived exosomes, suggesting that hsa-miR-4516 might be a pivotal regulator of exosome-mediated MSC-based therapeutics in regenerative medicine.

Recent studies have found that melatonin-induced MSC-derived exosomes enhance functional recovery in acute liver ischemia-reperfusion and renal ischemia-reperfusion injuries.[27,28] Similar to these findings, our study shows that MT exosome–treated CKD-MSCs improved neovascularization and functional recovery in a murine hindlimb ischemia model with CKD. MT exosomes increased the survival and proliferation of transplanted CKD-MSCs into ischemic sites by upregulating PrP^C. Taken together, the results indicate that MT exosomes enhance the regenerative potential of CKD-MSCs and treat CKD-mediated ischemic diseases via the miR-4516-PrP^C signaling cascade (Figure 8). We found that the transfer of PrP^C from MT exosomes to CKD-MSCs is an important intercellular communication mechanism that improves the functionality of CKD-MSCs. In conclusion, MT exosome–treated CKD-MSCs could be an efficacious cell-based therapeutic for patients with CKD.

ACKNOWLEDGEMENTS

The authors thank Mi Ra Yu in Dr Noh's laboratory for isolation of MSCs. This study was supported by the National Research Foundation grant funded by the Korean government (NRF-2017M3A9B4032528, NRF-2019M3A9H1103495). The funders had no role in the designing the study, data collection and analysis, decision to publish, and preparation of the manuscript.

CONFLICT OF INTEREST

The authors declare no conflict of interests.

AUTHOR CONTRIBUTIONS

YMY, JHL, and SHL conceived and designed the study, acquired and analyzed data, and drafted the manuscript. K-HS performed data acquisition, analysis interpretation, and statistical analysis. HN provided cells. Additionally, SHL procured the funding and provided feedback to the study.

ORCID

Sang Hun Lee https://orcid.org/0000-0002-6626-9702

REFERENCES

1. Peired AJ, Sisti A, Romagnani P. Mesenchymal stem cell-based therapy for kidney disease: a review of clinical evidence. *Stem Cells Int*. 2016;2016:4798639.
2. Stauffer ME, Fan T. Prevalence of anemia in chronic kidney disease in the United States. *PLoS ONE*. 2014;9(1):e84943.
3. Casiraghi F, Remuzzi G. Mesenchymal stromal cells in kidney transplantation. *Curr Opin Nephrol Hypertens*. 2019;28(1):40-46.
4. Schlieper G, Schurgers L, Brandenburg V, Reutelingsperger C, Floege J. Vascular calcification in chronic kidney disease: an update. *Nephrol Dial Transplant*. 2016;31(1):31-39.
5. Lisini D, Nava S, Pogliani S, et al. Adipose tissue-derived mesenchymal stromal cells for clinical application: an efficient isolation approach. *Curr Res Transl Med*. 2019;67(1):20-27.
6. Thery C, Ostrowski M, Segura E. Membrane vesicles as conveyors of immune responses. *Nat Rev Immunol*. 2009;9(8):581-593.
7. Lai RC, Yeo RW, Lim SK. Mesenchymal stem cell exosomes. *Semin Cell Dev Biol*. 2015;40:82-88.
8. Phinney DG, Pittenger MF. Concise review: MSC-derived exosomes for cell-free therapy. *Stem Cells*. 2017;35(4):851-858.
9. Boga JA, Caballero B, Potes Y, et al. Therapeutic potential of melatonin related to its role as an autophagy regulator: a review. *J Pineal Res*. 2019;66(1):e12534.
10. Yoon YM, Kim S, Han YS, et al. TUDCA-treated chronic kidney disease-derived hMSCs improve therapeutic efficacy in ischemic disease via PrP(C). *Redox Biol*. 2019;22:101144.
11. Lee JH, Han YS, Yoon YM, et al. Role of HSPA1L as a cellular prion protein stabilizer in tumor progression via HIF-1alpha/GP78 axis. *Oncogene*. 2017;36(47):6555-6567.
12. Han YS, Kim SM, Lee JH, Lee SH. Co-administration of melatonin effectively enhances the therapeutic effects of pioglitazone on mesenchymal stem cells undergoing indoxyl sulfate-induced senescence through modulation of cellular prion protein expression. *Int J Mol Sci*. 2018;19(5):E1367.
13. Yoon YM, Han YS, Yun CW, Lee JH, Kim R, Lee SH. Pioglitazone protects mesenchymal stem cells against p-cresol-induced mitochondrial dysfunction via up-regulation of PINK-1. *Int J Mol Sci*. 2018;19(10):E2898.
14. Han YS, Kim SM, Lee JH, Jung SK, Noh H, Lee SH. Melatonin protects chronic kidney disease mesenchymal stem cells against senescence via PrP(C) -dependent enhancement of the mitochondrial function. *J Pineal Res*. 2019;66(1):e12535.
15. Lee JH, Han YS, Lee SH. Potentiation of biological effects of mesenchymal stem cells in ischemic conditions by melatonin via upregulation of cellular prion protein expression. *J Pineal Res*. 2017;62(2):e12385.
16. Feng Y, Huang W, Wani M, Yu X, Ashraf M. Ischemic preconditioning potentiates the protective effect of stem cells through

secretion of exosomes by targeting Mecp2 via miR-22. *PLoS ONE*. 2014;9(2):e88685.
17. Liang X, Zhang L, Wang S, Han Q, Zhao RC. Exosomes secreted by mesenchymal stem cells promote endothelial cell angiogenesis by transferring miR-125a. *J Cell Sci*. 2016;129(11):2182-2189.
18. Xin H, Li Y, Liu Z, et al. MiR-133b promotes neural plasticity and functional recovery after treatment of stroke with multipotent mesenchymal stromal cells in rats via transfer of exosome-enriched extracellular particles. *Stem Cells*. 2013;31(12):2737-2746.
19. Katakowski M, Buller B, Zheng X, et al. Exosomes from marrow stromal cells expressing miR-146b inhibit glioma growth. *Cancer Lett*. 2013;335(1):201-204.
20. Iglesias DM, El-Kares R, Taranta A, et al. Stem cell microvesicles transfer cystinosin to human cystinotic cells and reduce cystine accumulation in vitro. *PLoS ONE*. 2012;7(8):e42840.
21. Katsuda T, Tsuchiya R, Kosaka N, et al. Human adipose tissue-derived mesenchymal stem cells secrete functional neprilysin-bound exosomes. *Sci Rep*. 2013;3:1197.
22. Amarnath S, Foley JE, Farthing DE, et al. Bone marrow-derived mesenchymal stromal cells harness purinergenic signaling to tolerize human Th1 cells in vivo. *Stem Cells*. 2015;33(4):1200-1212.
23. Liu Z, Gan L, Zhang T, Ren Q, Sun C. Melatonin alleviates adipose inflammation through elevating alpha-ketoglutarate and diverting adipose-derived exosomes to macrophages in mice. *J Pineal Res*. 2018;64(1):e12455.
24. Li X, Lv Y, Hao J, et al. Role of microRNA-4516 involved autophagy associated with exposure to fine particulate matter. *Oncotarget*. 2016;7(29):45385-45397.
25. Huang R, Yu T, Li Y, Hu J. Upregulated has-miR-4516 as a potential biomarker for early diagnosis of dust-induced pulmonary fibrosis in patients with pneumoconiosis. *Toxicol Res (Camb)*. 2018;7(3):415-422.
26. Cui T, Bell EH, McElroy J, et al. miR-4516 predicts poor prognosis and functions as a novel oncogene via targeting PTPN14 in human glioblastoma. *Oncogene*. 2019;38(16):2923-2936.
27. Sun CK, Chen CH, Chang CL, et al. Melatonin treatment enhances therapeutic effects of exosomes against acute liver ischemia-reperfusion injury. *Am J Transl Res*. 2017;9(4):1543-1560.
28. Alzahrani FA. Melatonin improves therapeutic potential of mesenchymal stem cells-derived exosomes against renal ischemia-reperfusion injury in rats. *Am J Transl Res*. 2019;11(5):2887-2907.

SUPPORTING INFORMATION

Additional supporting information may be found online in the Supporting Information section.

How to cite this article: Yoon YM, Lee JH, Song K-H, Noh H, Lee SH. Melatonin-stimulated exosomes enhance the regenerative potential of chronic kidney disease-derived mesenchymal stem/stromal cells via cellular prion proteins. *J Pineal Res*. 2020;68:e12632. https://doi.org/10.1111/jpi.12632